

TWO LAYER CONSTANT POWER CONTROL OF DFIG WIND TURBINES WITH SUPERCAPACITOR ENERGY STORAGE

A. Shiva kama Sundari^{*1}, D. Rajababu²

^{*1} PG [PE&ES] student, Department of EEE, S.R Engineering College, Telangana, India.

² Associate professor, Department of EEE, S.R Engineering College, Telangana, India.

ABSTRACT

To dynamically match the intermittency of wind energy, energy storage devices will be required. In this project a two-layer constant power control scheme for a wind farm equipped with doubly fed induction generator (DFIG) wind turbine is considered. In the two layer control, there is a high layer controller known as Wind farm supervisory control (WFSC), which generates Active power (P), Stator power (Ps), Energy storage power (Pe), DC voltage (Vdc) etc. references for the low layer Wind turbine generator (WTG) controllers, according to the power demand from the grid operator. The low layer wind turbine generator(WTG) controller consist of Rotor side converter control and Grid side converter control to regulate each Double fed induction generator (DFIG) wind turbine, to generate desired amount of active power, Where the deviations between the available wind energy input and desired active power output are compensated by Super capacitor Energy storage system. Simulation is carried out in a MATLAB/SIMULATION to evaluate the performance of wind farm equipped with 15 DFIG wind turbines with and without energy storage system to provide a constant active power of 36MW.

Keywords- Constant power control (CPC), Supercapacitor Energy storage system, Wind farm supervisory control, Wind Turbine Generator Contollers, doubly fed induction generator (DFIG).

1. INTRODUCTION

When wind turbines are connected to a grid, they should always maintain a constant power. In order to maintain a constant active power, the use of Double-Fed Induction generators(DFIG) with energy storage system like supercapacitors can be used with a two-layer constant power control scheme [1]. Wind turbine generators (WTGs) are usually controlled to generate maximum electrical power from wind under normal wind conditions. The European Wind Energy Association has set a target to satisfy more than 22% of European electricity demand with wind power by 2030 [2]. To enable WTGs to effectively participate in frequency and active power regulation, unit commitment, energy storage devices will be required to dynamically match the intermittency of wind energy [3]. Pumped water & compressed air are the most commonly used energy storage technologies for power grids due to their low capital costs [4]. Compared to batteries, supercapacitors have a higher power density, higher round-trip efficiency, longer cycle life, and lower capital cost per cycle [5]. This paper proposes considered a two-layer constant power control (CPC) scheme for a wind farm with a DFIG wind turbines.

2. SYSTEM DESCRIPTION

2.1 DFIG wind turbine with energy storage

Fig. 1 shows the basic configuration of a DFIG wind turbine equipped with a super capacitor-based ESS. The low-speed wind turbine drives a high-speed DFIG through a gearbox. The DFIG is a wound-rotor induction machine. It is connected to the power grid at both stator and rotor terminals. The stator is directly connected to the grid, while the rotor is fed through a variable-frequency converter, which consists of a rotor-side converter (RSC) and a grid-side converter (GSC) connected back to back through a dc link and usually has a rating of a fraction (25%–30%) of the DFIG nominal power.

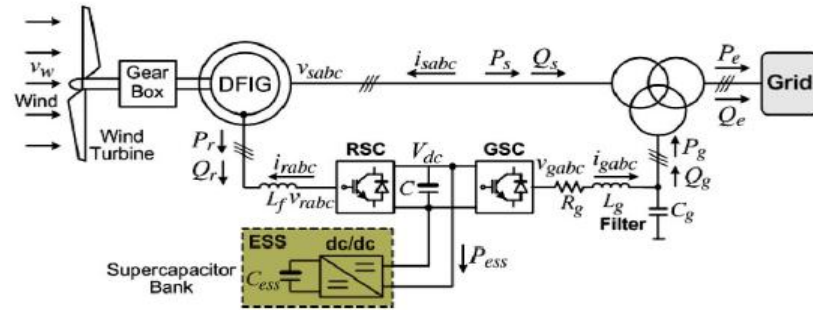


Fig -1: Configuration of a DFIG wind turbine equipped with an ESS connected to a grid.

An ESS consisting of a supercapacitor bank and a two-quadrant dc/dc converter is connected to the dc link of the DFIG converters. The ESS serves as either a source or a sink of active power and therefore contributes to control the generated active power of the WTG. The value of the capacitance of the supercapacitor bank can be determined by

$$C_{ess} = \frac{2P_n T}{V_{sc}^2} \tag{1}$$

2.2 Control of Individual DFIG Wind Turbine

2.2.1 Control of the RSC:

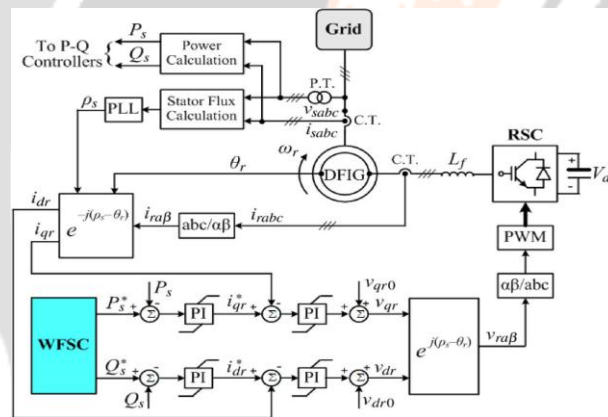


Fig -2: Overall vector control scheme of RSC

Fig. 2 shows the overall vector control scheme of the RSC, in which the independent control of the stator active power P_s and reactive power Q_s is achieved by means of rotor current regulation in a stator-flux oriented synchronously rotating reference frame. Therefore, the overall RSC control scheme consists of two cascaded control loops. The outputs of the two current controllers are compensated by the corresponding cross-coupling terms v_{dr0} and v_{qr0} , respectively, to form the total voltage signals v_{dr} and v_{qr} . They are then used by the PWM module to generate the gate control signals to drive the RSC.

2.2.2 Control of the GSC:

Fig. 3 shows the overall vector control scheme of the GSC, in which the control of the dc-link voltage V_{dc} and the reactive power Q_g exchanged between the GSC and the grid is achieved by means of current regulation in a synchronously rotating reference frame. Again, the overall GSC control scheme consists of two cascaded control loops. The outputs of the two current controllers are compensated by the corresponding cross coupling terms v_{dg0} and v_{qg0} , respectively, to form the total voltage signals v_{dg} and v_{qg} . They are then used by the PWM module to generate the gate control signals to drive the GSC. The reference signal of the outer-loop reactive power controller is generated by the high-layer WFSC.

power demand from or the generation commitment to the grid operator. The implementation of the WFSC is described by the flowchart in Fig: 6, where P_d is the active power demand from or the generation commitment to the grid operator; v_{wi} and V_{ess} are the wind speed in meters per second and the voltage of the supercapacitor bank measured from WTG i ($i = 1, \dots, N$), respectively; and N is the number of WTGs in the wind farm. Based on v_{wi} , the optimal rotational speed $\omega_{ti, opt}$ in radians per second of the wind turbine can be determined, which is proportional to the wind speed v_{wi} at a certain pitch angle β_i .

$$\omega_{ti, opt} = k(\beta_i)v_{wi} \quad (3)$$

Where k is a constant at a certain value of β_i , then the maximum mechanical power $P_{mi, max}$ that the wind turbine extracts from the wind can be calculated by the well-known wind turbine aerodynamic characteristics

$$P_{mi, max} = \frac{1}{2} \rho_i A_r v_{wi}^3 C_{Pi}(\lambda_{t, opt}, \beta_i) \quad (4)$$

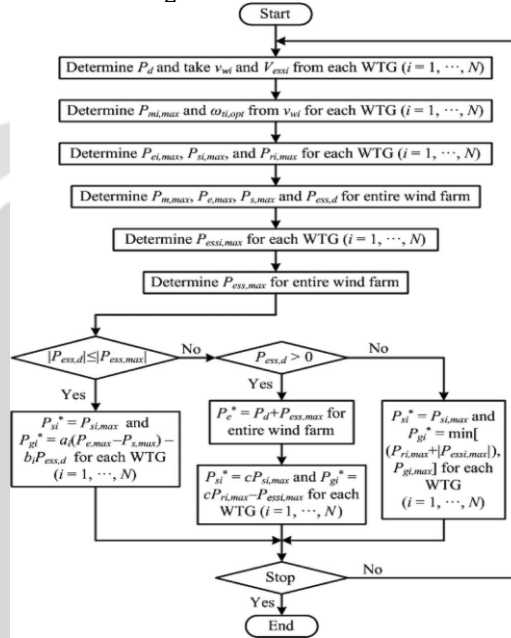


Fig -6: Flowchart of implementation of the WFSC

where ρ_i is the air density in kilograms per cubic meter; $A_r = \pi R^2$ is the area in square meters swept by the rotor blades, with R being the blade length in meters; and C_{Pi} is the power coefficient, which is a function of both tip-speed ratio λ_i and the blade pitch angle β_i , where λ_i is defined by

$$\lambda_i = \frac{\omega_{ti} R}{v_{wi}} \quad (5)$$

In (4), $\lambda_{i, opt}$ is the optimal tip-speed ratio when the wind turbine rotates with the optimal speed $\omega_{ti, opt}$ at the wind speed v_{wi} . Given $P_{mi, max}$, the maximum active power $P_{ei, max}$ generated by the WTG can be estimated by taking into account the power losses of the WTG

$$P_{ei, max} = P_{mi, max} - P_{Li} = P_{si, max} + P_{ri, max} \quad (6)$$

Where P_{Li} is the total power losses of WTG i , which can be estimated by the method in; $P_{si, max}$ and $P_{ri, max}$ are the maximum DFIG stator and rotor active powers of WTG i , respectively. The stator active power P_s can be written in a synchronously rotating dq reference frame as follows:

$$P_s = \frac{3}{2} (v_{ds} i_{ds} + v_{qs} i_{qs}) \approx \frac{3}{2} [\omega_s L_m (i_{qs} i_{dr} - i_{ds} i_{qr}) + r_s (i_{ds}^2 + i_{qs}^2)] \quad (7)$$

where v_{ds} and v_{qs} are the d - and q -axis voltage components of the stator windings, respectively; i_{ds} and i_{qs} are the stator d - and q -axis current components, respectively; i_{dr} and i_{qr} are the rotor d - and q -axis current components, respectively; ω_s is the rotational speed of the synchronous reference frame; and r_s and L_m are the stator resistance and mutual inductance, respectively. Similarly, the rotor active power is calculated by

$$P_r = \frac{3}{2} (v_{dr} i_{dr} + v_{qr} i_{qr}) \approx \frac{3}{2} [-s \omega_s L_m (i_{qs} i_{dr} - i_{ds} i_{qr}) + r_r (i_{dr}^2 + i_{qr}^2)] \quad (8)$$

where v_{dr} and v_{qr} are the d - and q -axis voltage components of the rotor windings, respectively; s is the slip of the DFIG defined by

$$s = (\omega_s - \omega_r) / \omega_s \quad (9)$$

where ω_r is the DFIG rotor speed. (7) And (8) yield

$$s = -\frac{P_r - 3i_r^2 r_r}{P_s - 3i_s^2 r_s} \tag{10}$$

Where

$$i_s = \sqrt{i_{ds}^2 + i_{qs}^2} / 2 \text{ and } i_r = \sqrt{i_{dr}^2 + i_{qr}^2} / 2$$

If neglecting the stator copper loss $3i_s^2 r_s$ and rotor copper loss $3i_r^2 r_r$ of the DFIG, the relationship between the stator and rotor active powers can be approximated by

$$P_r = -sP_s \tag{11}$$

According to (6) and (10) [or (11)], $P_{si,max}$ and $P_{ri,max}$ of each WTG can be determined.

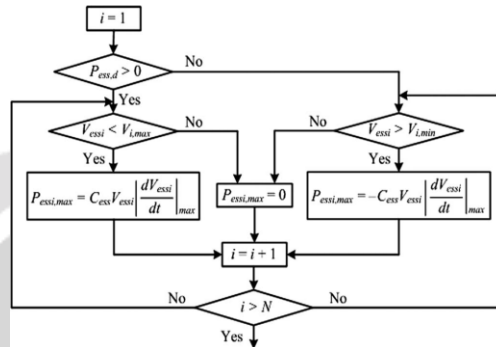


Fig -7: Flowchart of determination of $P_{ess,i,max}$ for each WTG

Then, the total maximum mechanical power $P_{m,max}$, DFIG output active power $P_{e,max}$, and stator active power $P_{s,max}$ of all WTGs in the wind farm can be calculated as

$$P_{m,max} = \sum_{i=1}^N P_{mi,max} \tag{12}$$

$$P_{e,max} = \sum_{i=1}^N P_{ei,max} \tag{13}$$

$$P_{s,max} = \sum_{i=1}^N P_{si,max} \tag{14}$$

In order to supply constant power P_d to the grid, the deviation $P_{ess,d}$ between the demand/commitment P_d and the maximum generation $P_{e,max}$ is the power that should be stored in or supplied from the ESSs of the WTGs

$$P_{ess,d} = P_{e,max} - P_d \tag{15}$$

During normal operation, $V_{ess,i}$ must be maintained within the following range:

$$V_{i,min} < V_{ess,i} < V_{i,max} \tag{16}$$

The maximum power $P_{ess,i,max}$ that can be exchanged between the supercapacitor bank and the DFIG dc link of WTG i can be determined by

$$P_{ess,i,max} = \pm C_{ess} V_{ess,i} \left| \frac{dV_{ess,i}}{dt} \right|_{max} \tag{17}$$

Where $|dV_{ess,i}/dt|_{max}$ is the maximum rate of voltage variations of the supercapacitor bank, which is related to the current limits of the supercapacitor bank. In (17), the positive sign indicates storing energy, while the negative sign indicates supplying energy by the ESS. The calculation of $P_{ess,i,max}$ for each WTG is subjected to (16). Fig: 7 shows how to determine $P_{ess,i,max}$ for each WTG. If $P_{ess,d} > 0$, extra power needs to be stored in the ESSs. In this case, if $V_{ess,i} < V_{i,max}$, $P_{ess,i,max}$ is calculated by (17) and takes the positive sign; otherwise, the ESS cannot store any power and $P_{ess,i,max} = 0$. On the contrary, if $P_{ess,d} < 0$, active power needs to be supplied from the ESSs. In this case, if $V_{ess,i} > V_{i,min}$, $P_{ess,i,max}$ is calculated by (17) and takes the negative sign; otherwise, the ESS cannot supply any power and $P_{ess,i,max} = 0$. As shown in Fig: 6, once $P_{ess,i,max}$ of each WTG is determined, the total maximum power $P_{ess,max}$ that can be exchanged between the supercapacitor bank and the DFIG dc link of all WTGs can be determined by

$$P_{ess,max} = \sum_{i=1}^N P_{ess,i,max} \tag{18}$$

Finally, depending on the relationship of $P_{ess,d}$ and $P_{ess,max}$, the reference signals P_{si}^* (see Fig:5.2) and P_{gi}^* (see Fig:5.4) of each WTG can be determined. Specifically, if $|P_{ess,d}| \leq |P_{ess,max}|$, P_{si}^* and P_{gi}^* can be determined directly, as shown in Fig:5.6, where the partition coefficients a_i 's are calculated by

$$a_i = \frac{P_{ri,max}}{P_{e,max} - P_{s,max}} \tag{19}$$

and the partition coefficients b_i 's are calculated by

$$b_i = \frac{P_{essi,max}}{P_{ess,max}} \tag{20}$$

The coefficients a_i and b_i have the following feature:

$$\sum_{i=1}^N a_i = 1 \quad \sum_{i=1}^N b_i = 1 \tag{21}$$

If $|P_{ess,d}| > |P_{ess,max}|$, depending on the sign of $P_{ess,d}$, P_{si}^* and P_{gi}^* can be determined, as shown in Fig. 6. If $P_{ess,d}$ is positive, the ESSs of the WTGs store active power, and the total active power generated by all DFIGs is P_{e}^* , which is less than $P_{e,max}$. Therefore, a scaling factor c is defined as follows:

$$c = \frac{P_{e}^*}{P_{e,max}} \tag{22}$$

and P_{si}^* and P_{gi}^* can be determined by using the scaling factor. If $P_{ess,d}$ is negative, the ESSs of the WTGs supply active power, the RSC of each WTG is controlled to generate the maximum stator active power $P_{si,max}$, and the ESS of each WTG is controlled to generate active power of P_{gi}^* ,

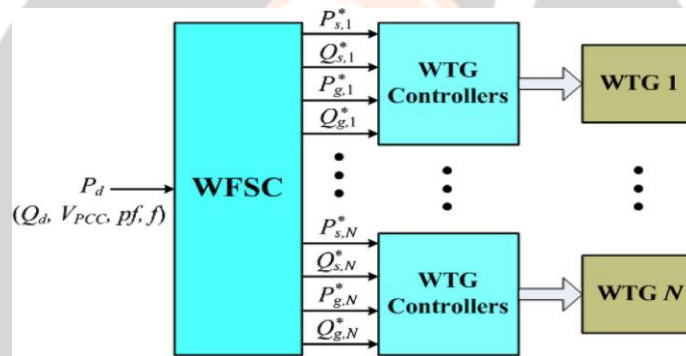


Fig -8: proposed two-layer CPC scheme for the wind farm.

Fig. 8 shows the block diagram of the proposed two-layer CPC scheme for the wind farm. In practice, the value of P_d should take into account the generation capability of the wind farm and should be subjected to the following limit:

$$P_d \leq \bar{P}_{e,max} \tag{23}$$

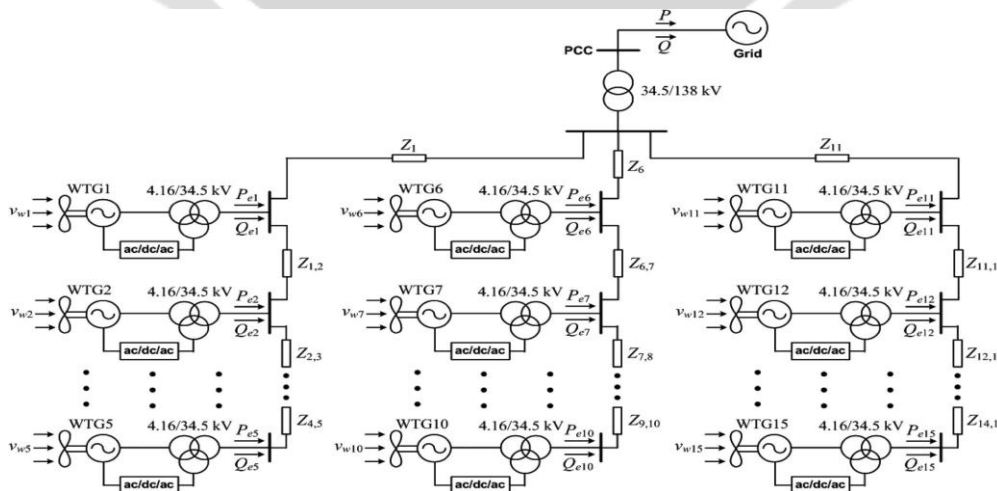


Fig -9: Configuration of a wind farm equipped with 15 DFIG wind turbines connected to a grid.

The reactive power references of the RSC and GSC controllers can be determined by controlling the power factor (pf) or the voltage (VPCC) at the point of common coupling (PCC) of the wind farm at the desired value or to supply a desired amount of reactive power as required by the grid operator.

4. SIMULATION RESULTS

Simulation studies are carried out for a wind farm with 15 DFIG wind turbines to verify the effectiveness of the proposed control scheme under various operating conditions. Each DFIG wind turbine has a 3.6MW power capacity. The total power capacity of the wind farm is 54 MW.

4.1 CPC During Variable Wind Speed Conditions

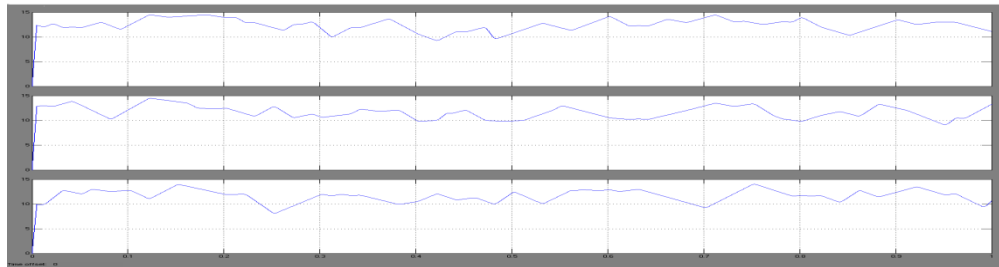


Fig: 10 Wind speed profiles of WTG1, WTG6, and WTG11

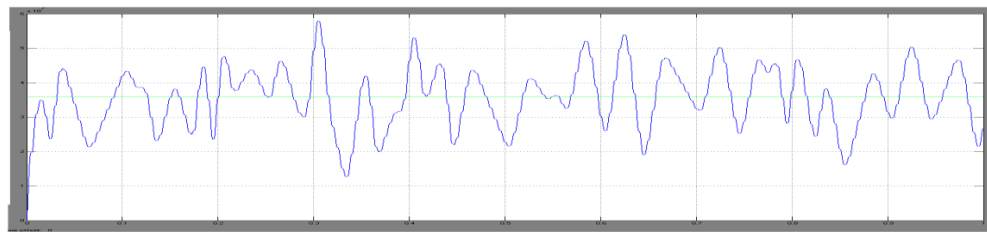


Fig: 11 Comparison of the wind farm power output and constant power demand Without ESS

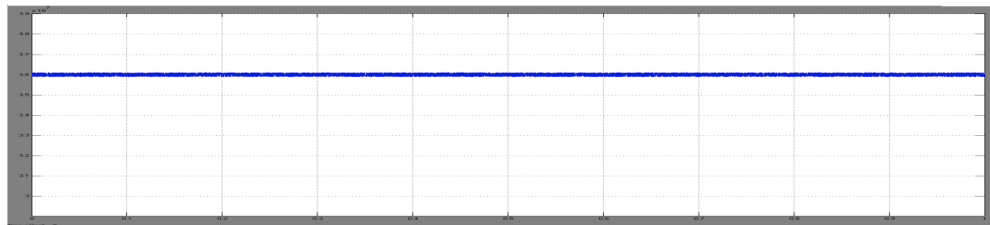


Fig: 12 Comparison of the wind farm power output and the constant power demand from or commitment to the grid operator: With ESSs and the proposed CPC scheme.

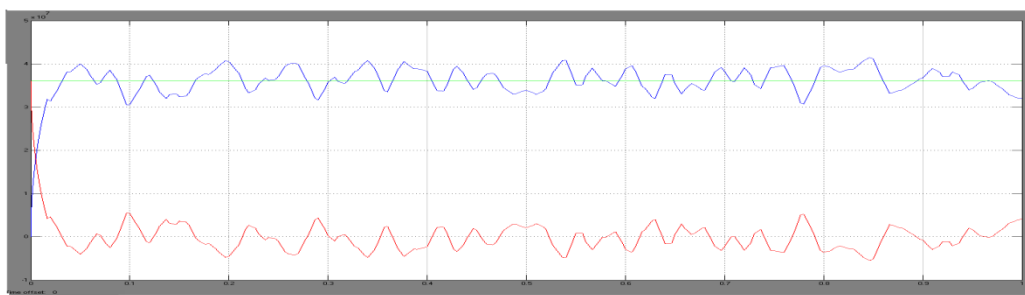


Fig: 13 Active powers of all WTGs and the wind farm

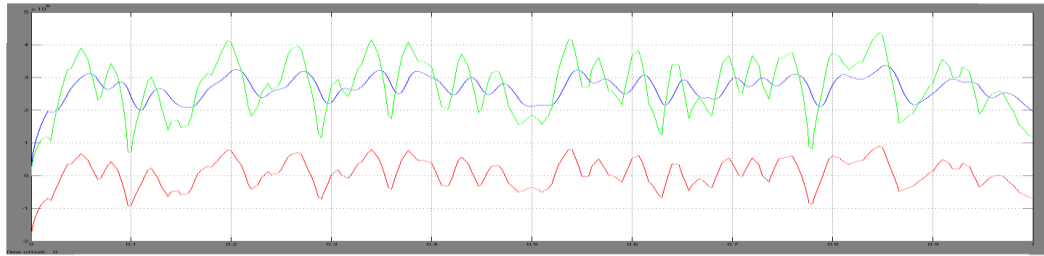


Fig: 14 Stator active power (P_{s1}), GSC active power (P_{g1}) & total active power output (P_{e1}) of WTG1.

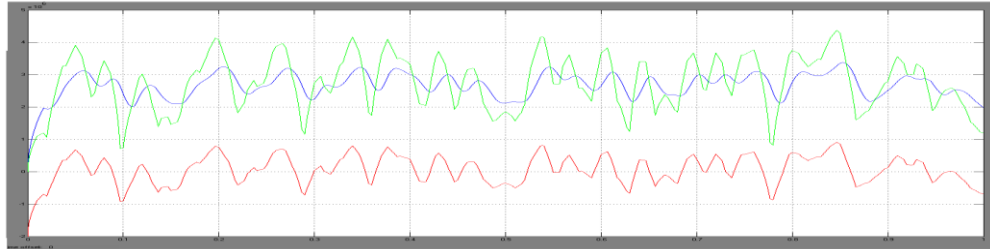


Fig: 15 Stator active power (P_{s6}), GSC active power (P_{g6}) & total active power output (P_{e6}) of WTG6

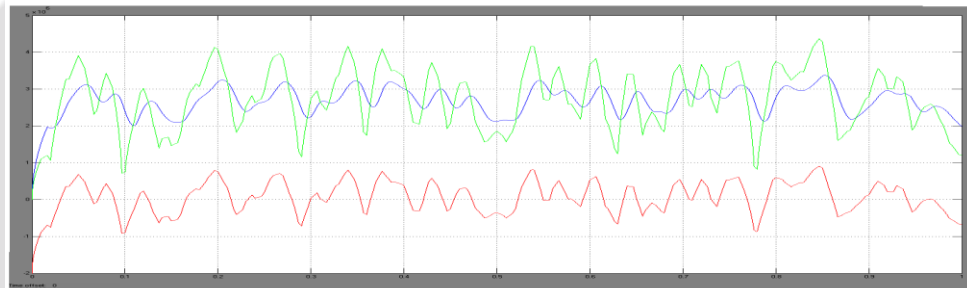


Fig 16 Stator active power (P_{s11}), GSC active power (P_{g11}) & total active power output (P_{e11}) of WTG11

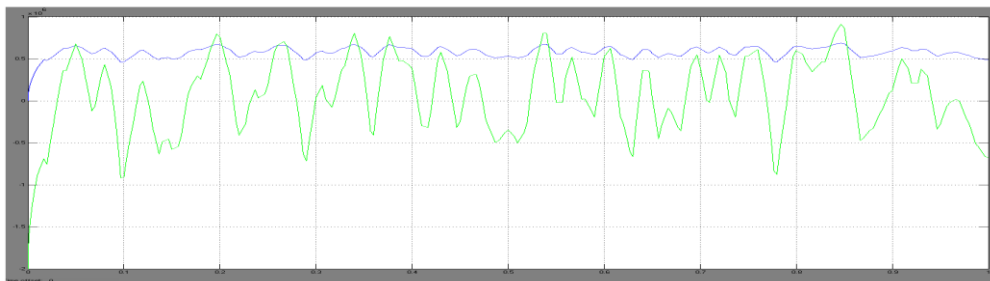


Fig 17 Rotor active power (P_{r1}) & active power stored/supplied by the ESS (P_{ess1}) of WTG1

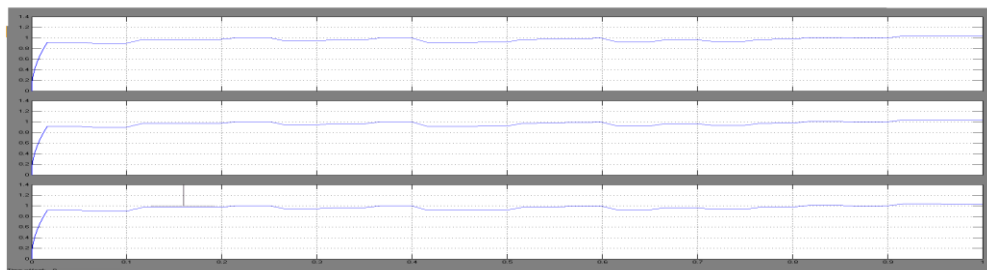


Fig: 18 Voltages of the supercapacitor banks of WTG1, WTG6, and WTG11

4.2 Power Tracking During Step Changes in Demand/Commitment

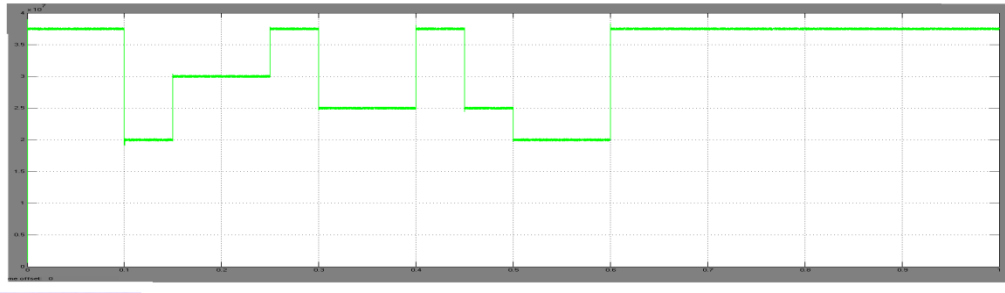


Fig.19 Power tracking performance of the wind farm during step changes in demand from or commitment to the grid operator

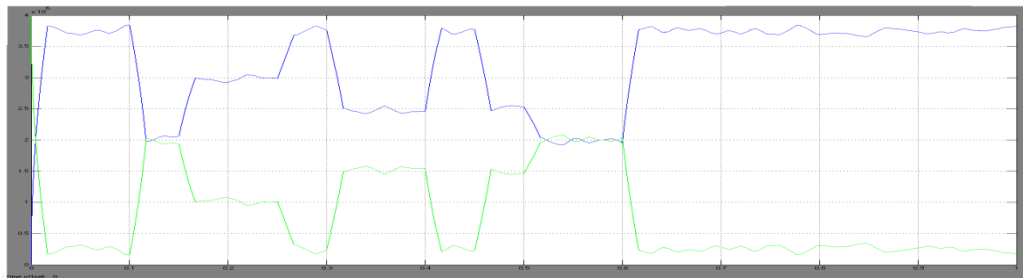


Fig. 20 Total active power outputs of WTG1 (Pe1) and WTG5 (Pe5) during step changes in demand from or commitment to the grid operator

5. CONCLUSION

In this paper, a two-layer Constant Power Control scheme for a wind farm equipped with 15 DFIG wind turbine is considered. The WFSC generates the active power references for the low-layer WTG controllers according to the active power demand from or generation commitment to the grid operator; the low-layer WTG controllers then regulate each DFIG wind turbine to generate the desired amount of active power, where the deviations between the available wind energy input and desired active power output are compensated by the ESS.

In this paper, Energy storage system serves as either a source or a sink of active power to control the generated active power of the DFIG wind turbine. Power electronic devices Rotor side converter, Grid side converter and DC/DC converter are promising technical solutions to provide wind power installations with power system control capabilities and to improve their effect on power system stability. Simulation studies are carried out in MATLAB/SIMULATION on a wind farm equipped with 15 DFIG wind turbines to verify the effectiveness of the proposed control scheme.

6. FUTURE SCOPE

This project has unlocked many gates for the future young engineers to install the wind power plants to fulfill the gap between the current power generations and future power demand needed. Now the penetration of wind power to the power grids is 1-2% of nations power by the use of advanced energy storage devices like Supercapacitors we can achieve 20% of wind power in nation's total power by 2030.

REFERENCES

- [1]. Liyan Qu, *Member, IEEE*, and Wei Qiao, *Member, IEEE*, "Constant Power Control of DFIG Wind Turbines With Supercapacitor Energy Storage" VOL. 47, NO. 1, JANUARY/FEBRUARY 2011.
- [2]. "Focus on 2030: EWEA aims for 22% of Europe's electricity by 2030," *Wind Directions*, pp. 25–34, Nov./Dec. 2006.
- [3]. J. P. Barton and D. G. Infield, "Energy storage and its use with intermittent renewable energy," *IEEE Trans. Energy Convers.*, vol. 19, no. 2, pp. 441–448, Jun. 2004.

- [4]. D. Rastler, "Electric energy storage, an essential asset to the electric enterprise:Barriers and RD&D needs," *California Energy Commission Staff Workshop Energy Storage Technol., Policies Needed Support California's RPS Goals 2020*, Sacramento, CA, Apr. 2, 2009.
- [5]. C. Abbey and G. Joos, "Supercapacitor energy storage for wind energy applications," *IEEE Trans. Ind. Appl.*, vol. 43, no. 3, pp. 769–776, May/June. 2007.
- [6]. W. Qiao, W. Zhou, J. M. Aller, and R. G. Harley, "Wind speed estimation based sensorless output maximization control for a wind turbine driving a DFIG," *IEEE Trans. Power Electron.*, vol. 23, no. 3, pp. 1156–1169, May 2008.
- [7]. W. Qiao, G. K. Venayagamoorthy, and R. G. Harley, "Real-time implementation of a STATCOM on a wind farm equipped with doubly fed induction generators," *IEEE Trans. Ind. Appl.*, vol. 45, no. 1, pp. 98–107, Jan./Feb. 2009.
- [8]. A. Yazdani, "Islanded operation of a doubly-fed induction generator (DFIG) wind-power system with integrated energy storage," in *Proc. IEEE Canada Elect. Power Conf.*, Montreal, QC, Canada, Oct. 25–26, 2007, pp. 153–159.
- [9]. 20% Wind Energy By 2030: Increasing Wind Energy's Contribution to U.S. Electricity Supply, U.S. Department of Energy, Jul. 2008.
- [10]. W. Qiao and R. G. Harley, "Grid connection requirements and solutions for DFIG wind turbines," in *Proc. IEEE Energy Conf.*, Atlanta, GA, Nov. 17–18, 2008, pp. 1–8.

BIOGRAPHIES



A. Shiva kama sumdhari received the B.Tech degree from jayamuki institute of technological sciences, Warangal affiliated to JNTU-Hyderabad. Present she is perceive M.Tech[power engineering and Energy system] from S.R.engineering college(autonomous), Warangal. Her research areas includes power balancing of hybrid renewable energy system with power system automation.



D. Rajababu received the B.Tech in Electrical and Electronics Engineering in JNTU,Ananthapur in the year of 1999 and M.Tech in electrical power systems in JNTU,Ananthapur in the year of 2002. Currently, he is associate of Electrical and Electronics Engineering, S.R. Engineering college. His areas of interest include Voltage and frequency control of wind power stations.